Measurement of the Moisture Content in Woodchips Through Capacitive Sensing and Data Driven Modelling

Authors: Wenbiao Zhang [a] (Corresponding author)

Jing Yan [a]

Yong Yan [b]

Addresses: [a] School of Control and Computer Engineering

North China Electric Power University

Beijing 102206

P. R. China

Tel: +86 01061771330

Email: wbzhang@ncepu.edu.cn

[b] School of Engineering and Digital Arts

University of Kent

Canterbury

Kent CT2 7NT

UK

Abstract

In this paper, a helical capacitive sensor is developed to measure the moisture content (MC) in woodchips. Firstly, based on the orthogonal test method, the structure of the capacitive sensor is optimized to obtain the best possible uniform sensitivity. Then, the effect of the type and random distribution of woodchips on the capacitive MC measurement is investigated. Finally, three different algorithms, including support vector machine, random forest and deep neural network, are employed to establish the data driven models. Experimental results demonstrate that the proposed system is capable of measuring the MC in woodchips with absolute error within ±5%. The generalization capability is verified using the cedarwood with three size ranges, with R^2, RMSE and MAE of 0.95, 1.69% and 1.28%, respectively. The absolute error of the predicted MC in cedarwood over the range 24.3% and 25.2% is found to be within ±2% for a range of packing densities.

Keywords – Moisture content measurement, data driven modelling, helical capacitive sensor, finite element modelling, woodchips.

1. Introduction

As a renewable and carbon neutral biomass material, woodchips are widely applied in power plants and domestic boilers for the power generation and heating. The moisture content (MC) is an important factor that affects the mechanical performance and physical stability of the woodchips. The MC of woodchips depends on many factors, such as the age, species and cutting season of the tree. Before the combustion of woodchips, they are usually squashed and compressed. However, woodchips with exceedingly high or very low MC cannot be molded. Moreover, in the combustion process, a higher MC consumes extra energy in the furnace, which results in lower combustion efficiency [1]. Therefore, accurate and reliable MC measurement is needed for woodchips.

The MC in woodchips (W_0) reported in this work is the gravimetric MC and it is defined as:

$$W_0 = \frac{m_w - m_d}{m_w} \times 100\% \quad (1)$$

where m_d and m_w are the mass of dried and wet woodchips, respectively [1].

The available methods to measure the MC in woodchips mainly include direct and indirect methods. The oven drying method is considered as a direct method. Material is dried at a high temperature until the weight reaches a constant weight. The oven drying method is time-consuming and destructive, so it is not suitable for online continuous measurement and large-scale usage. Although this method has above shortcomings, the MC from the oven drying method is often used as the reference value.

Near-infrared spectroscopy (NIR), microwave, X-ray, nuclear magnetic resonance (NMR), imaging processing and electrical methods are usually considered as indirect methods. NIR method applies reflectance and absorbance principles and the amplitude ratio of the reflected wavelengths between the reference and sample beams is used to calculate the MC [2]. However, NIR method measures the MC of thin materials and only the moisture on material's surface is detected. In addition, the effects of material size, surface characteristics and surface color result in measurement errors. Microwave sensors have been used to measure the MC in different materials and the microwave method is independent of density changes [3-5]. In addition, several new algorithms are proposed for the MC prediction. However, because of the higher operation frequency, the measurement system for the microwave method is more complex. X-ray and NMR methods estimate the MC from the attenuation coefficient of the X-ray beams and NMR signal [6, 7]. However, X-ray and NMR methods are extremely expensive and have limited accessibility due to potential radiation hazard. The MC can also be measured using the image processing method and it is predicted by establishing the relationship between image characteristics and the MC [8].

However, the image processing method needs a homogenous surface and rough surfaces or variations in color result in large errors.

Since the MC affects electrical properties such as resistivity or dielectric property of the material, the electrical method usually includes resistive and capacitive methods [9, 10]. The resistance of dry material is higher than that of water. The higher the MC, the lower the resistance value is. There is a quantitative relationship between the MC and the resistance value. However, when the MC of the material is low, the resistance value is extremely high, which results in difficulty to measure the MC accurately. For capacitive method, dry wood has the relative permittivity between 2 and 4 and water at ambient temperature has the relative permittivity of about 80 [10]. Because of the large difference in the dielectric property, the variations in MC cause obvious changes in the capacitance, which results in high sensitivity for MC measurement. In addition, the capacitive method has the advantages of non-destructiveness, simple structure, and good repeatability.

Different types of electrodes are adopted for the capacitive MC measurement, which include parallel plate electrode [11-13], interdigital electrode [14, 15], fringing-field electrode [16, 17] and multi-electrode [18]. However, parallel plate, interdigital and fringing-field electrodes have non-uniform sensitivity distribution due to the fringe field effect. The capacitive measurement of the MC will be affected because of the random packing of woodchips in the sensing volume. Moreover, the sensor with multiple electrodes takes a long time in each MC measurement cycle. Many factors such as type, packing density and particle size of woodchips are not comprehensively analyzed for the capacitive MC measurement. Traditionally, the MC measurement was conducted by establishing empirical equations, which build the relationship between the MC and electrical parameters of impedance, capacitance and phase angle [11]. However, these equations have poor generalization capability.

In this paper, the capacitive sensing and data driven modelling is combined to predict the MC in woodchips. The proposed method can estimate the MC in different kinds of woodchips under different packing densities using a simply and low cost capacitive measurement system. The main contributions include three points:

1) A helical capacitive sensor, which has relatively more uniform sensitivity than its counterparts [19-22], is applied and the structural parameters of the sensor are optimized.

2) The capacitance spectrum obtained through the frequency sweeping is introduced and various factors on the capacitive MC measurement are experimentally investigated.

3) Since data driven modelling has many advantages in solving complex and non-linear problems with good generalization capability [23], data driven models based on support vector machine (SVM), random forest (RF) and deep neural network (DNN) are established to predict the MC in woodchips. Comparative assessments and comprehensive evaluation of the data driven models for the MC prediction in applewood and cedarwood with three size ranges are conducted.

2. Methodology

2.1 Measurement Principle

The measurement principle of the proposed method is given in Fig. 1. Compared with the single frequency and two-frequency measurement, the application of multiple frequencies provides more information of the dielectric property [24]. For example, different types of woodchips have different dielectric properties and their capacitance spectra can help to improve the prediction accuracy of the MC in woodchips. Therefore, the capacitive sensing system in this paper applies the frequency sweeping method to obtain the capacitance spectrum of woodchips. Moreover, in view of its advantages of high prediction accuracy and good generalization capability, data driven modelling is adopted to predict the MC in this study. By investigating the characteristics of the capacitance

spectrum and the influence of the type and random distribution of woodchips in the sensor, the signal features from the capacitance spectrum and the mass of the sample are selected to be the input of data driven models. SVM, RF and DNN algorithms are selected to build data driven models for the prediction of the MC in woodchips and the reason for choosing these three algorithms is that they have different features. SVM is a supervised learning algorithm that is widely used for the classification or regression problems. Due to the features of fast response and simple structure, data driven models based on SVM have been applied to predict the MC in the soil and fresh fruits [25, 26]. RF is created based on the bootstrapping of many decision trees and the final prediction of the RF model is obtained by averaging the response from all the trees. The features of RF model include high prediction accuracy, high tolerance for noise data and outliers, and low possibility to overfitting [27]. With the popularity of deep learning, deep learning algorithms have been widely applied in data driven modelling [28, 29]. DNN is a type of feed forward neural network, which has more than one hidden layer. Compared with shallow learning algorithms, the deeper architecture of DNN increases the prediction accuracy and improves the generalization capability to new samples [30].

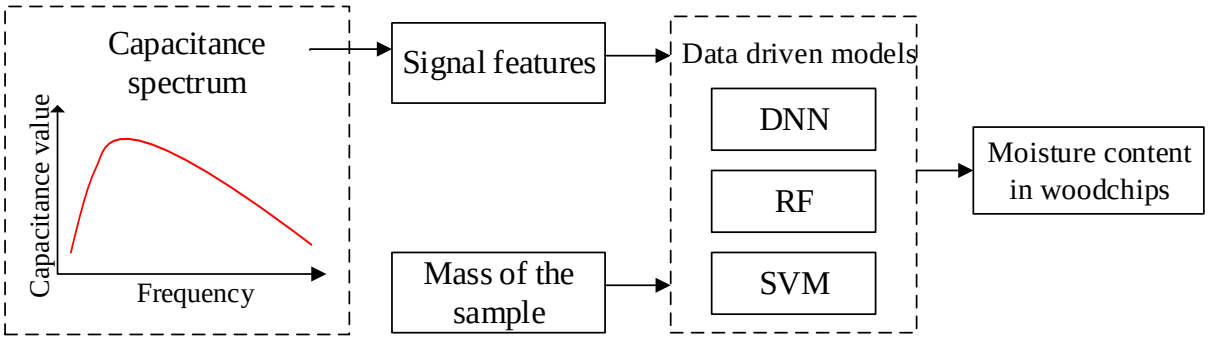

Fig. 1. Schematic diagram of the measurement principle.

2.2 Sensor Design

As shown in Fig. 2, the helical capacitive sensor includes a detection electrode, a source electrode and two types of shielding electrode. The stray capacitance and fringe field effect can be reduced by the edge guard electrode and the electromagnetic noise can be eliminated by the shielding electrode.

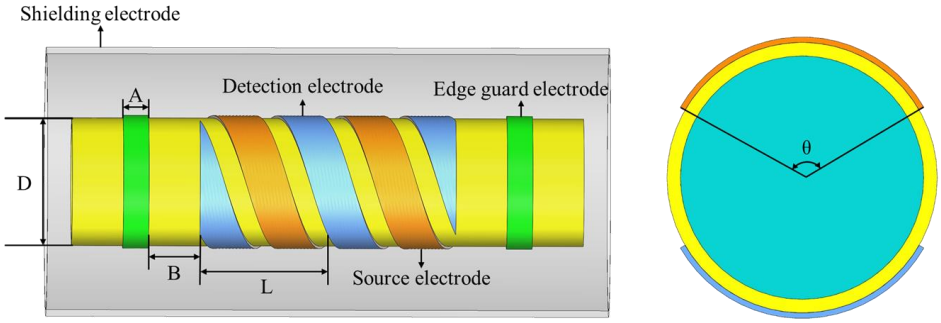

Fig.2. Structure of the helical capacitive sensor.

The structural parameters of the sensor are shown in Fig. 2, where L is the axial length of the helical electrode, A is the width of the edge guard electrode, B is the axial distance between the source electrode and edge guard electrodes, θ is the plate opening angle. These structural parameters affect the sensitivity distribution of the helical sensor and they should be optimized [18]. Because it is complex and impractical to determine the electrostatic field analytically, the optimization of the sensor structure is accomplished by a finite element model (FEM). Since the random packing of woodchips in the capacitive sensor will affect the optimization results, for the purpose of the sensitivity distribution optimization, there is no need to consider the target material to be measured. Considering only the air and water, the optimization of the sensor structure can also be realized. During the simulation, 10×10 elements are created in the sensing volume. The material in each element is set as water and air respectively, to investigate the sensitivity distribution of the helical sensor. The sensitivity of the helical sensor is defined as:

$$S_t(i) = \frac{C_i - C_l}{C_h - C_l} \times \frac{V}{V_i} \tag{2}$$

where i represents the sequence number of the sensing element in the FEM model. $S_t(i)$ denotes the sensitivity of the ith element. C_h and C_l are the capacitance values when the sensing volume is full of water and air, respectively. C_i is the capacitance value when the material of the ith element is set as water, while the rest volume is set as air. V_i is the volume of the ith sensing element and V is the whole sensing volume.

Non-uniformity S_r is used as the objective function for the sensor optimization.

$$S_{\mathrm{r}} = \frac{S_\sigma}{\overline{S}} \tag{3}$$

where S_σ and $\overline{S}$ are the variation and average of the sensitivity value in the sensing volume, respectively. Thus, the smaller the S_r is, the more uniform the sensitivity will be.

The orthogonal experimental design is a widely used multi-factor experimental method based on an orthogonal array and it has already been used to optimize the sensor structure [18]. Based on the orthogonality, some representative points are selected from comprehensive experiments, which gives equivalent results in the minimum number of attempts. The different levels for structural parameters of the helical capacitive sensor are given in Table 1. In order to extend the simulation results to the helical sensor with different diameters, L, A and B are normalized to the outer diameter of the pipe (D) [18]. Since D is just a coefficient, the normalization will not affect the optimal values of L, A and B.

Table 1. Levels of four structure parameters for the capacitive sensor

Levels	Parameters			
	L/D	*θ (°)*	*A/D*	*B/D*
I	1	90	0.25	0.25
II	3	110	0.5	0.5
III	5	130	0.75	0.75
IV	7	150	1	1

The orthogonal table based on four parameters and their four possible levels, which need 16 experimental runs, are given in Table 2. The last column of Table 2 shows the corresponding S_r to the related experiment runs. The average S_r is calculated for each parameter under four levels. Fig. 3 shows the relationship between the average S_r and the parameters of *L/D*, θ, *A/D* and *B/D*. The course of the curves between the points is calculated through cubic spline data interpolation. It is found that the change in *L* causes the most obvious variation in average S_r. It's proved that *L* has the largest influence on the sensitivity distribution of the sensor, followed by *A* and *B*, while θ has a smaller impact. The results suggest that the larger the parameters *L*, *B* and *A* are, the more uniform the sensitivity distribution will be. In fact, it is impractical for the sensor with a long axial length. Moreover, when the *L/D* is larger than 3, the change of average S_r becomes smaller. Considering all the structural parameters and the practicality of the sensor, the parameters are *L/D*=3, θ=110 °, *A/D*=0.6 and *B/D*=0.5, respectively. The sensitivity distribution test of the parameters is also conducted and the resulting S_r is 0.32. Since the sensing volume of the optimized helical sensor is not perfectly uniform, the random distribution of woodchips in the sensor still leads to errors in the MC measurement.

Table 2. L16(4^4) Orthogonal table and simulation results

Configuration	Parameter levels				S_r
	L/D	*Θ*	*A/D*	*B/D*	
1	I	I	I	I	0.93
2	I	II	II	II	0.73
3	I	III	III	III	0.69
4	I	IV	IV	IV	0.70
5	II	I	II	III	0.50
6	II	II	I	IV	0.56
7	II	III	IV	I	0.52
8	II	IV	III	II	0.55
9	III	I	III	IV	0.38

10	III	II	IV	III	0.37
11	III	III	I	II	0.52
12	III	IV	II	IV	0.53
13	IV	I	IV	II	0.32
14	IV	II	III	I	0.37
15	IV	III	II	IV	0.38
16	IV	IV	I	III	0.47

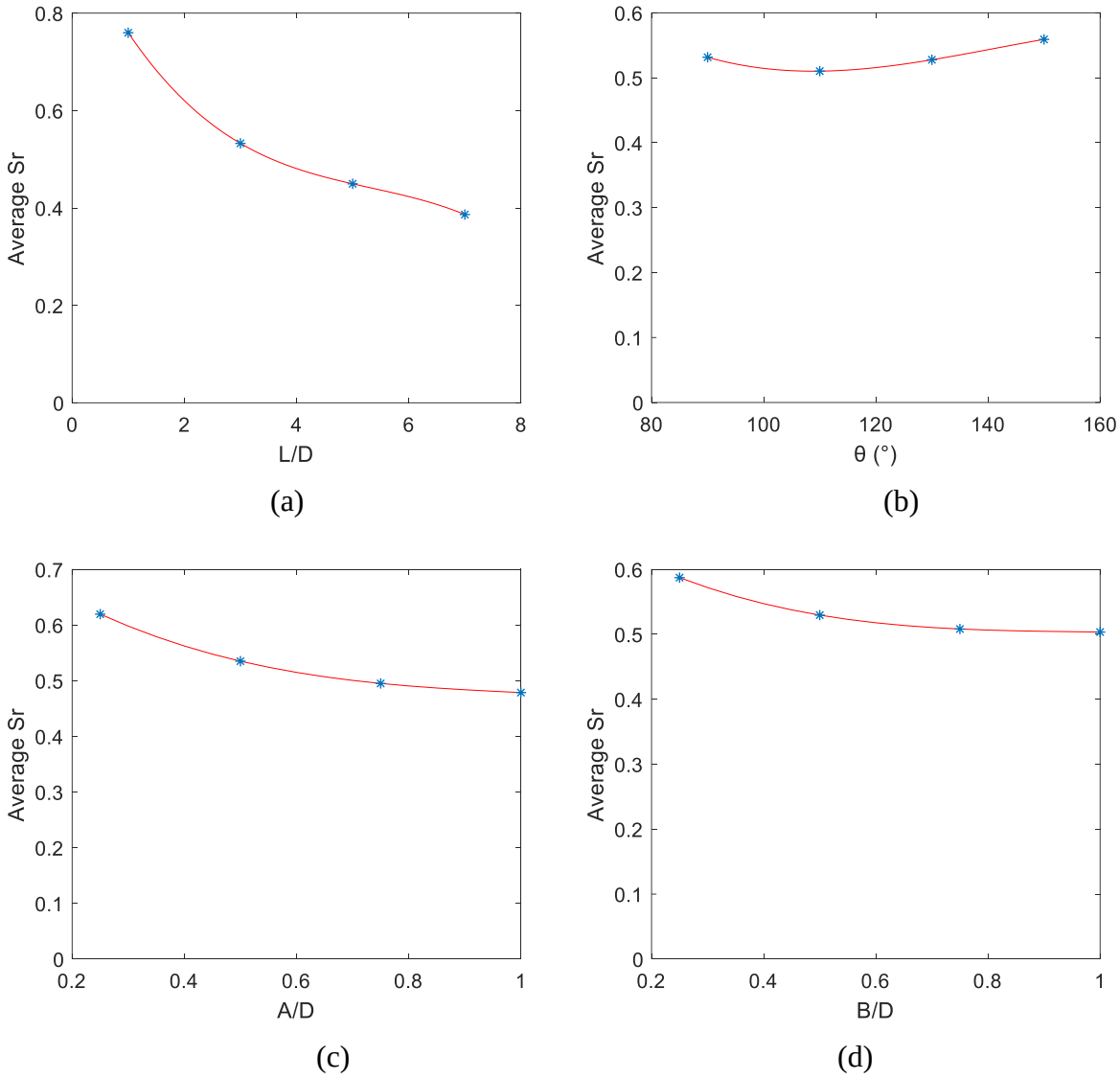

Fig. 3. Average S_r versus structural parameters. (a) *L/D*. (b) θ. (c) *A/D*. (d) *B/D*.

3. Experimental setup

3.1. Measurement System

The measurement system as shown in Fig. 4, includes a helical capacitive sensor, a LCR meter (Keysight E4980AL) and a personal computer (Intel Core i5 1.80 GHz with 12 GB of RAM). The LCR meter sweeps from 20 Hz to 1MHz and a capacitance spectrum with 201 points is obtained. In each MC measurement, the MATLAB program that is developed in-house sends control commands to the LCR meter to obtain the capacitance spectrum from the sensor and reads the mass of the sample from the precision electronic scale. The signal features of the capacitance spectrum and the mass of the sample are input into the data driven models and the predicted MC in woodchips is calculated. In addition, the reference MC in woodchips is obtained by a halogen analyzer (Mettler HE83). The equipment applies the oven drying method over the drying temperature from 50 to 200 ^{o}C. The repeatability of the equipment with 10g sample is 0.05% with the MC ranging from 1% to 100%.

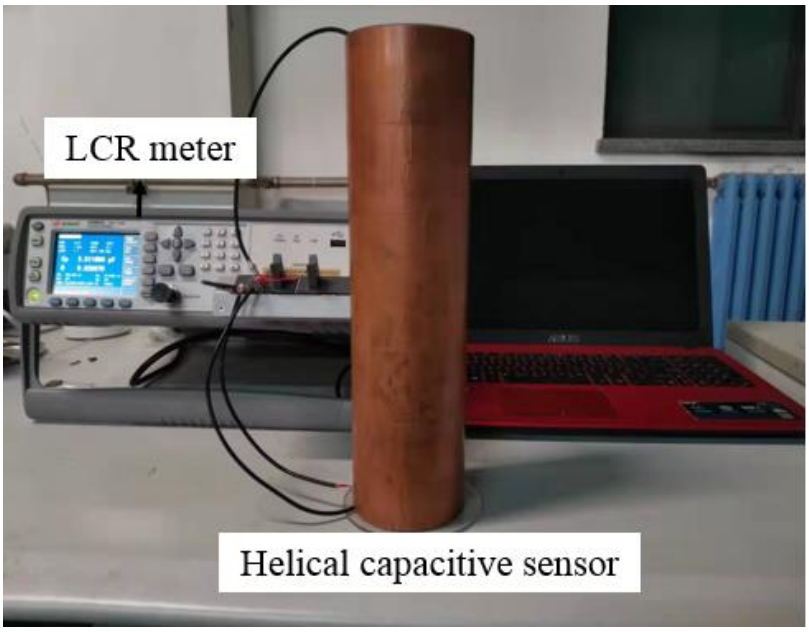

Fig. 4. Experimental setup.

3.2. Samples and Experimental Procedure

Two types of woodchips, applewood and cedarwood, were used in the experimental investigations. The true densities of applewood and cedarwood are 0.83 and 0.54 kg/m^3, respectively, which are provided by the supplier. The true densities are the mass of woodchips divided by the volume without voidage. In addition, for each type of woodchips, small, medium and large samples were tested. Their sizes are 0.5-1 cm,1.5-2.5 cm and 3-5 cm, respectively. Fig. 5 shows the images of the three sized applewood woodchips.

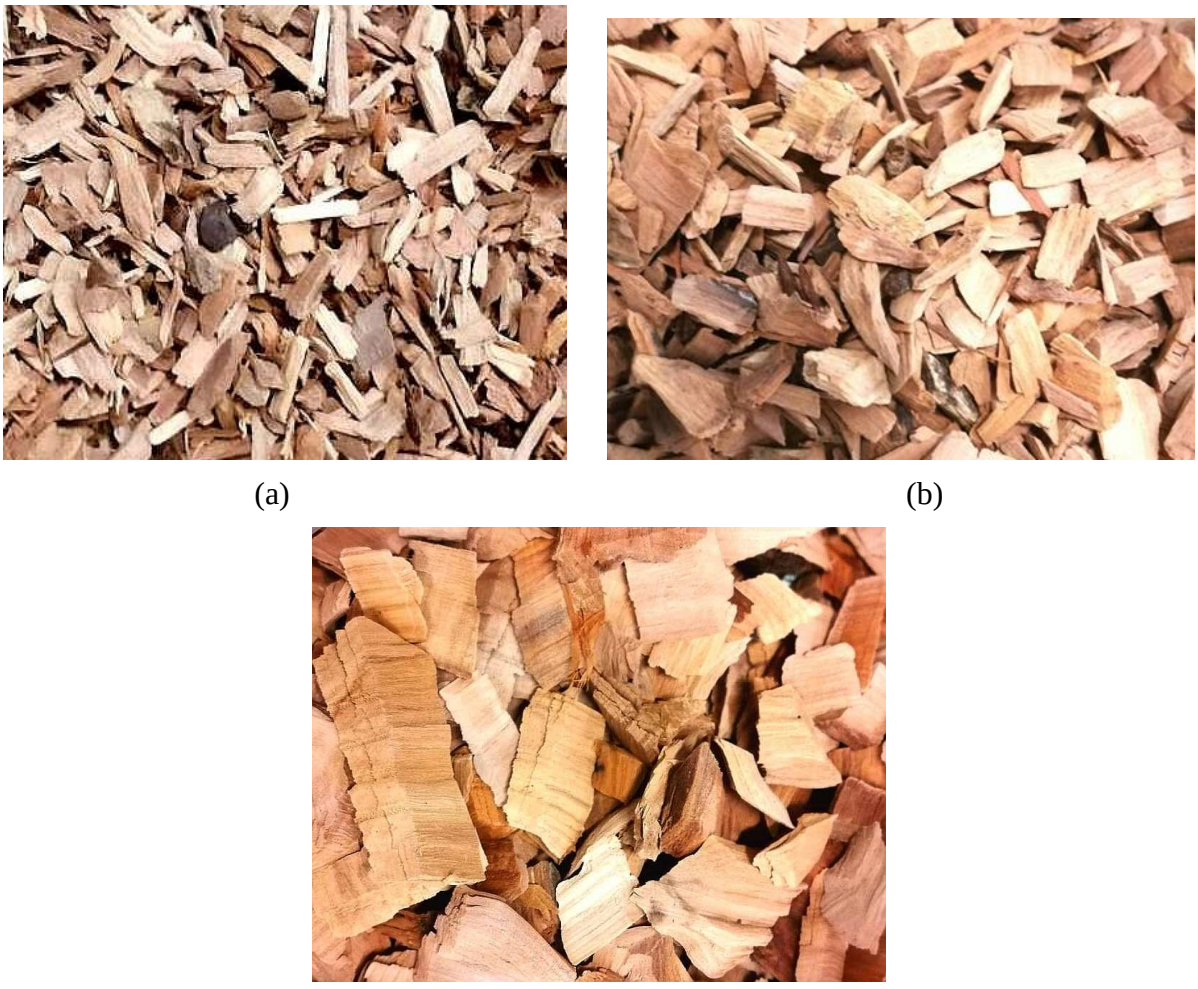

(a) (b)

(c)

Fig. 5. Applewood woodchips. (a) Small samples. (b) Medium samples. (c) Large samples.

Before the experiments, the woodchips were ventilated on a metal plate for a few days to maintain nearly consistent initial MC in each woodchip. These woodchips were separated into 15

groups and placed in plastic bottles. By adding a certain amount of water to each bottle, 15 different levels of MC were obtained during the experiments. Since the range of the MC in woodchips for the industry varies from 10% to 45% [1], the MC in the experiments was set between 7% and 49% with a 3% increment. These woodchips were firstly placed for a few days and shook periodically to ensure the homogeneity of moisture distribution in the bottle. Next, the prepared woodchips were put into the capacitive sensor and the corresponding capacitance values were recorded. Finally, three sub-groups of woodchips were randomly selected from each bottle and their MC were measured using the halogen analyzer. The average value was calculated as the reference MC. In addition, the capacitance spectrum was measured for three times under each MC measurement. Fig. 6 shows the capacitance spectra from three test runs with small sized cedarwood when the MC is 11.47%, 23.47% and 47.41%, respectively. When the frequency is greater than 100 Hz, the maximum discrepancy among the capacitance values from the three runs is 0.82 pF, 1.33 pF and 1.52 pF, respectively. In addition, with the increase of the frequency, the discrepancy becomes smaller, showing the repeatability of the capacitive sensing system. By averaging the results from the three runs, the capacitance spectrum for each MC is obtained.

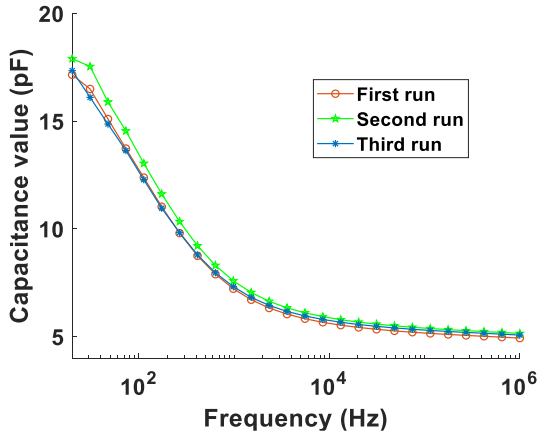

(a)

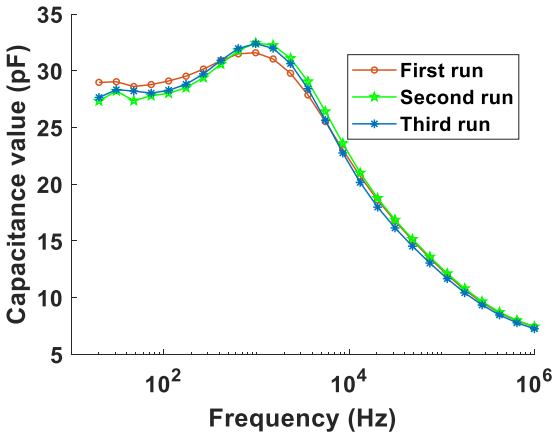

(b)

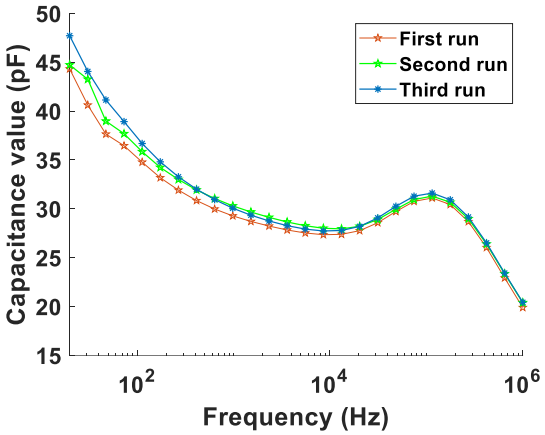

(c)

Fig. 6. Capacitance spectra from three test runs with small sized cedarwood for different MC. (a) MC of 11.47%. (b) MC of 21.86%. (c) MC of 47.41%.

4. Experimental results and discussion

4.1. Frequency Sweeping Results

The capacitance values under different frequencies with different MC are shown in Fig. 7. It is found that the capacitance value decreases monotonically with the increase of frequency under lower MC (lower than 20%). In addition, a crest appears when the MC increases to about 20%. The dielectric constant in the material is determined by the polarization effect and the dipole is randomly arranged under the normal condition. The arrangement of the dipole reverses with the variation in the electric field. With the increase of the frequency, the polarization effect intensifies and the capacitance value increases. However, because of the internal resistance of the material, the reversal arrangement of the dipole cannot keep up with the variation in the electric field under high frequency. The polarization effect weakens and the capacitance value decreases [31]. As a result, a peak appears in the capacitance spectrum.

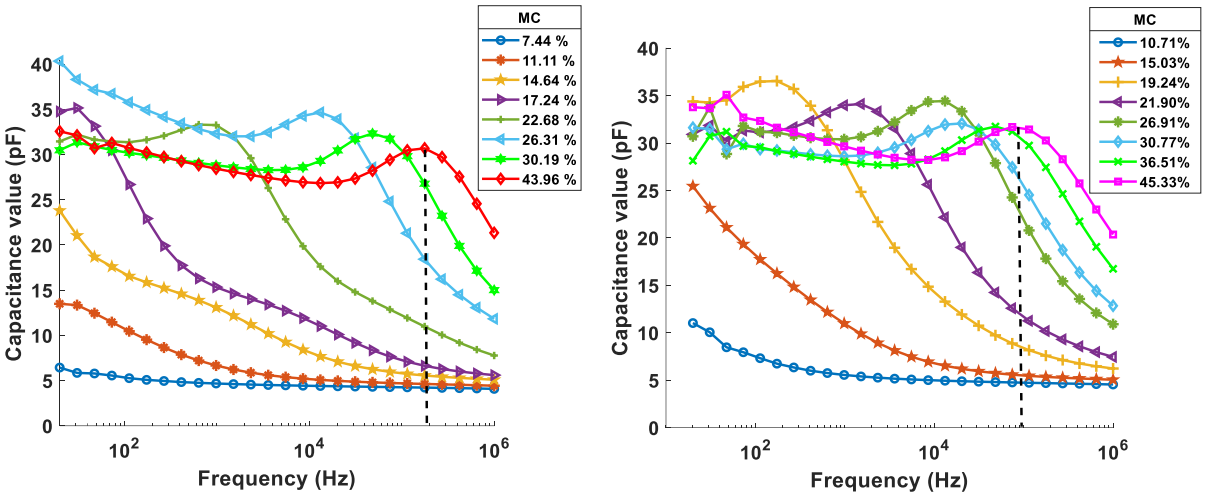

(a) (b)

Fig. 7. Capacitance spectra with different MC. (a) Small sized applewood. (b) Small sized cedarwood.

The capacitance value and corresponding frequency at the peak of capacitance spectrum are recorded to explore whether the peak is related to the MC in woodchips. Their quantitative relationships are given in Fig. 8. The results show that there is a good correlation between the frequency and the MC. Therefore, it can be used for the capacitive MC measurement. However, there is no obvious correlation between the capacitance value and the MC. Moreover, the corresponding data from the cedarwood samples have similar results. The reason for the monotonous relationship between the frequency and the MC is that the polarization effect is affected by the frequency of the electric field and the largest polarization effect occurs in woodchips with different MC under different frequencies of the electric field.

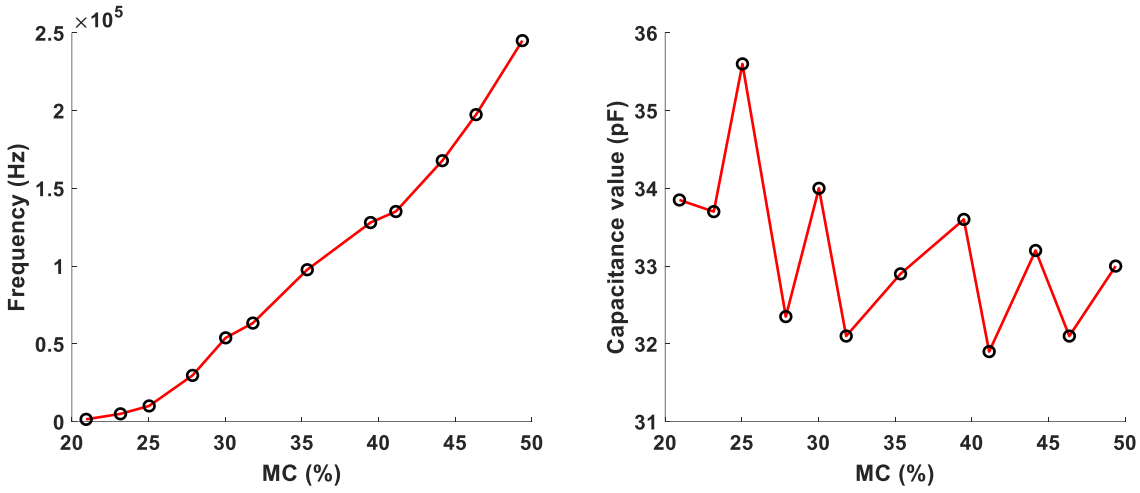

(a) (b)

Fig. 8. Relationship of the frequency at the peak and the corresponding capacitance value with the MC. (a) Frequency at the peak. (b) Capacitance value at the peak.

4.2. Different Types of Woodchips

Different types of woodchips have obvious difference in density. Fig. 9 (a) is a comparison of the capacitance spectrum of small sized applewood and cedarwood when the MC is 16.55%. As shown in the figure, at a certain frequency, the capacitance value is lower when the woodchip has lower density and this phenomenon is more obvious when the frequency is lower. The reason is that when the density of woodchips increases, the number of dipoles per unit volume increases and the polarization effect of woodchips intensifies, thus resulting in the increase of the capacitance value. In addition, there are also apparent differences in the frequency values at the peak under different types of woodchips, as shown in Fig. 9 (b). As a result, more features are needed to predict the MC in different types of woodchips.

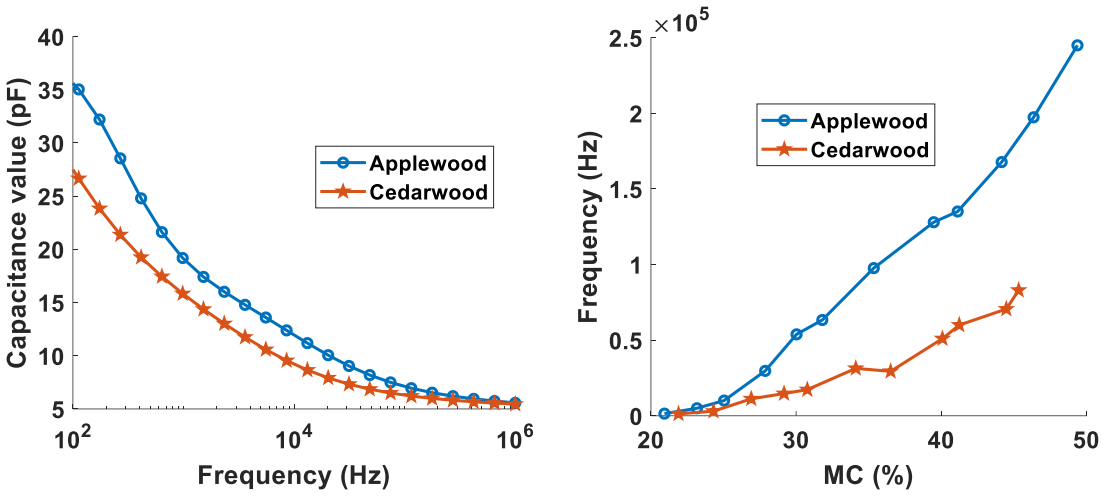

(a) (b)

Fig. 9. Comparison of different types of woodchips. (a) Capacitance spectrum. (b) Frequency at the peak.

4.3. Random Distribution of Woodchips

Random distribution of woodchips in the sensor is investigated in two aspects: Firstly, the distribution of woodchips is affected by the particle size. Different particle sizes lead to different distributions. Under the same type of woodchips, a larger particle size results in a smaller packing density. As a result, the effect of particle size needs to be considered in the capacitive MC measurement. Secondly, the packing of woodchips in the sensor is quite random and the packing density of woodchips varies in each measurement even for the same particle size. In order to investigate the influence of packing density, variable mass of woodchips is put into the sensor in each experiment, resulting in different mass within the same packing volume. The mass value of the sample is recorded to represent its packing density. The capacitance spectra when the MC is 14.03%, 25.04%, 39.48% and 49.48%, respectively are given in Fig. 10. The samples investigated are applewood woodchips with small particle size under different packing densities. It is found that the curves follow the same trend under different MC and the capacitance value increases with the packing density. Moreover, the peak points in the capacitance spectrum shift to the right. As a

consequence, the packing density of woodchips has a great influence on the capacitive MC measurement and the mass of the sample needs to be an input for data driven models.

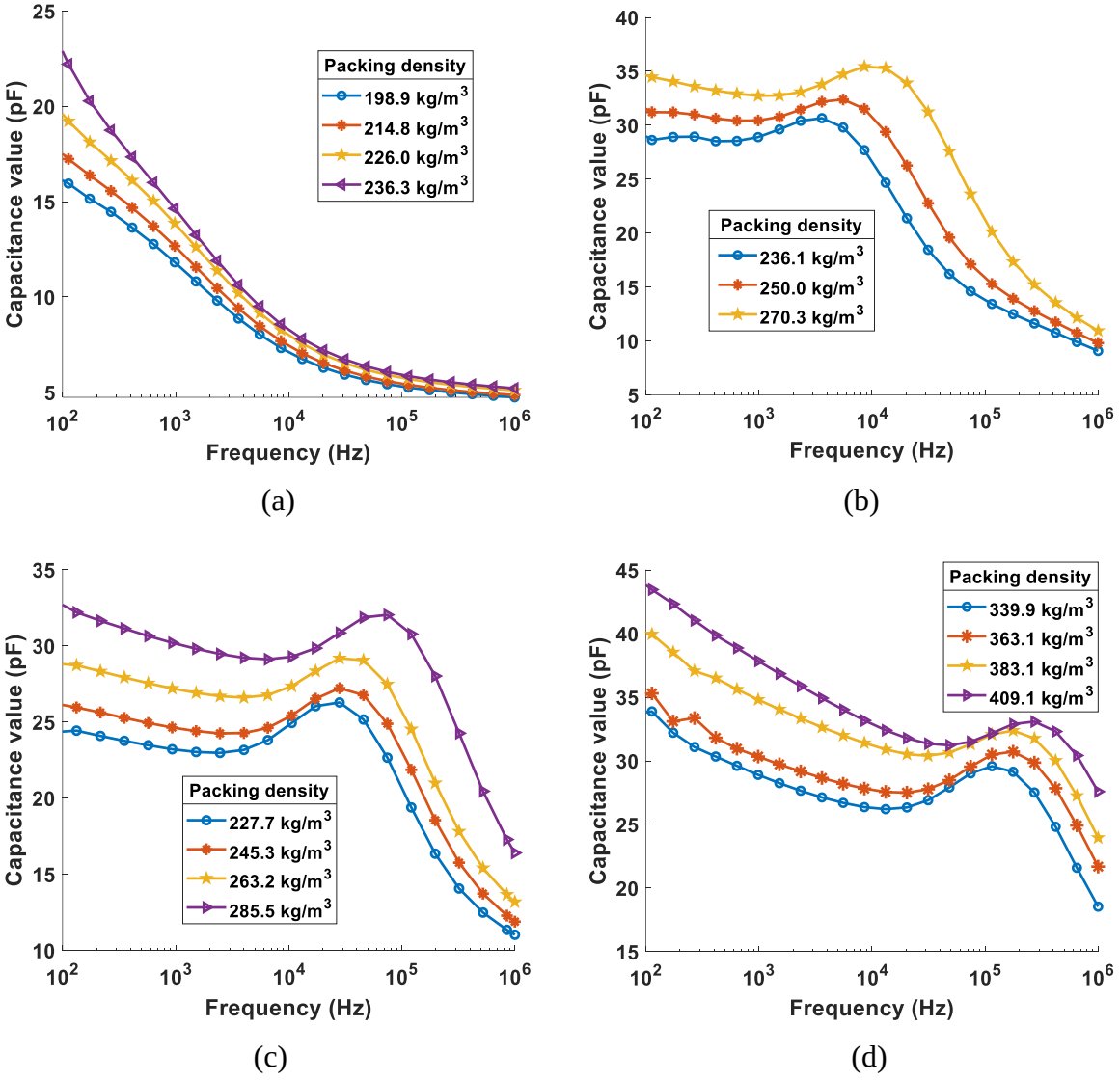

Fig. 10. Capacitance spectra of small sized applewood under different MC and packing densities. (a) MC of 14.03%. (b) MC of 25.04%. (c) MC of 39.48%. (d) MC of 49.48%.

4.4. Capacitance Values Under Different Frequencies

The capacitance values of woodchips under different frequencies are also analyzed. As shown in Fig. 7, when the frequency of the electric field is larger than the maximum frequency at the peak of the capacitance spectrum (black dash line in Fig. 7), the capacitance value increases monotonically

with the MC. Within the MC range investigated in this paper, the maximum frequency at the peak of the capacitance spectrum is 293 kHz when the MC of applewood is 49.48%. By analyzing the relationships between capacitance values under different frequencies and the MC, as given in Fig. 11, the capacitance value between 300 kHz and 1 MHz can be the input of data driven models. In addition, it has been proved that variations in the dielectric property at different frequencies can be used to predict the MC of grain and nuts and the greater the difference in the dielectric property, the more sensitive the prediction model will be [11]. Therefore, the capacitance values at 300 kHz and 1 MHz are selected for the MC prediction in this paper.

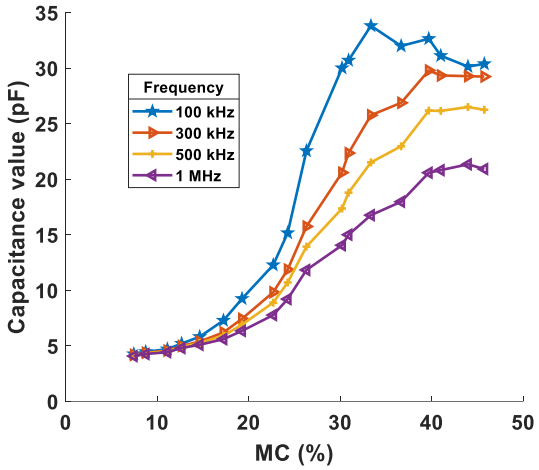

Fig. 11. Relationship between the capacitance values under different frequencies and the MC in woodchips.

4.5. Data Driven Modelling for Capacitive MC Measurement

Based on the above experimental investigations, the mass of the sample, the frequency at the peak of the capacitance spectrum and the capacitance values at 300 kHz and 1 MHz are selected as the input of data driven models. In addition, when there is no peak in the capacitance spectrum, the frequency is set to 0. Three data driven models using SVM, RF and DNN algorithms are built. The criteria for the selection of the hyper-parameters of the data driven models are given as follows:

The DNN model used in this paper contains 4 hidden layers and the number of neurons in each layer is 10, 6, 6 and 4, respectively. It is found that, when the number of hidden layers is higher than 4, the prediction accuracy of the MC is almost the same. In view of the prediction accuracy and model complexity, the DNN model with 4 hidden layers are developed. Bayesian hyper-parameter optimization is carried out for the RF model [32]. The optimum parameters are selected that the number of tree is 120, the minimum number of samples in the leaf node is 3 and the maximum number of features is 2. The penalty parameters of the SVM model are optimized through five-fold cross validation and the kernel function is set as the cubic polynomial kernel after comprehensive comparisons. The coefficient of determination (R^2), the root mean square error (RMSE), the mean absolute error (MAE) and the prediction time (T) are used to investigate the performance of data driven models.

$$R^2 = \frac{(\sum_{i=1}^{n}(P_i - \bar{P})(R_i - \bar{R}))^2}{\sum_{i=1}^{n}(P_i - \bar{P})^2 \sum_{i=1}^{n}(R_i - \bar{R})^2} \tag{4}$$

$$RMSE = \sqrt{\frac{\sum_{i=1}^{n}(P_i - R_i)^2}{n}} \tag{5}$$

$$MAE = \frac{\sum_{i=1}^{n}|P_i - R_i|}{n} \tag{6}$$

where R_i and P_i are the reference and predicted values of MC, respectively, $\bar{R}$ and $\bar{P}$ are the averages of the reference and predicted values, respectively, and n is the number of samples in the dataset.

70% of the data from the applewood are randomly selected as a training dataset and the remaining data are used as a validation dataset. Three data driven models mentioned above are trained and

validated using the personal computer. The validation results of the data driven models are shown in Fig. 12. The results from the proposed model are the average of DNN and SVM models. It is found all the data driven models can predict the MC in woodchips with absolute error within ±5%. In addition, as given in Fig. 12, most of prediction results have the absolute error within ±2%. For example, 90% of prediction results from the proposed model (Fig. 12 (d)) have the absolute error within ±2%. The main reason for the error is the sensitivity distribution of the sensor, which is not perfectly uniform. The performance of the data driven models is listed in Table 3. DNN and SVM models have similar prediction accuracy, while the RF model has the largest error. The reason is that although the final prediction of the RF model is calculated by averaging the results from all trees, the unexpected prediction from a single tree results in the larger error of the MC measurement. In addition, since DNN and SVM models have different features, a combination of the two models makes the proposed model more accurate. By averaging the results from DNN and SVM models, the proposed model has the higher prediction accuracy with RMSE and MAE of 1.21% and 0.99%, respectively.

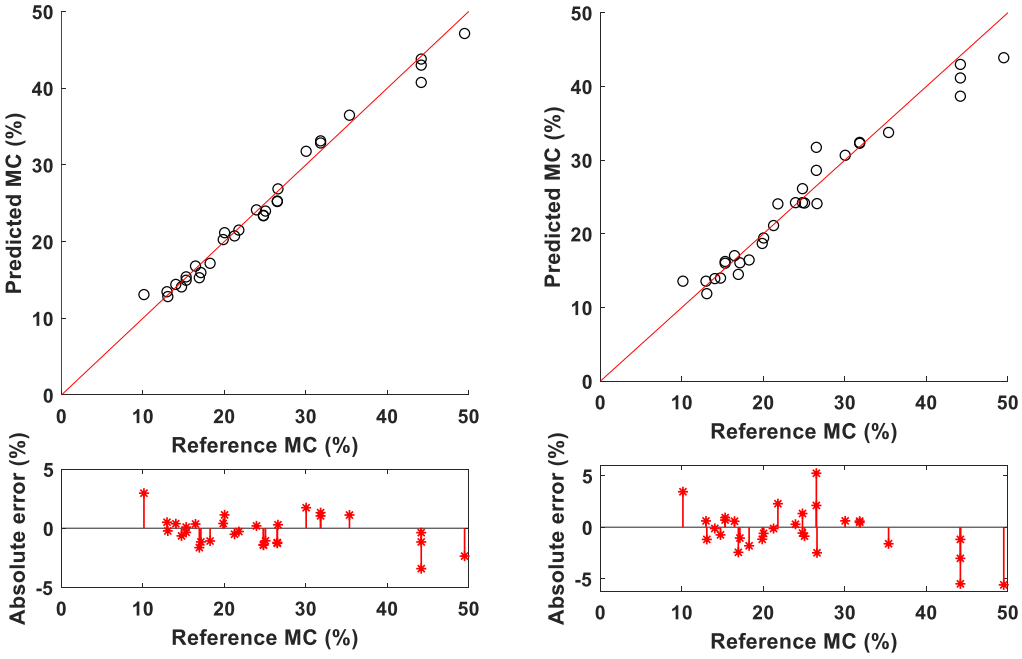

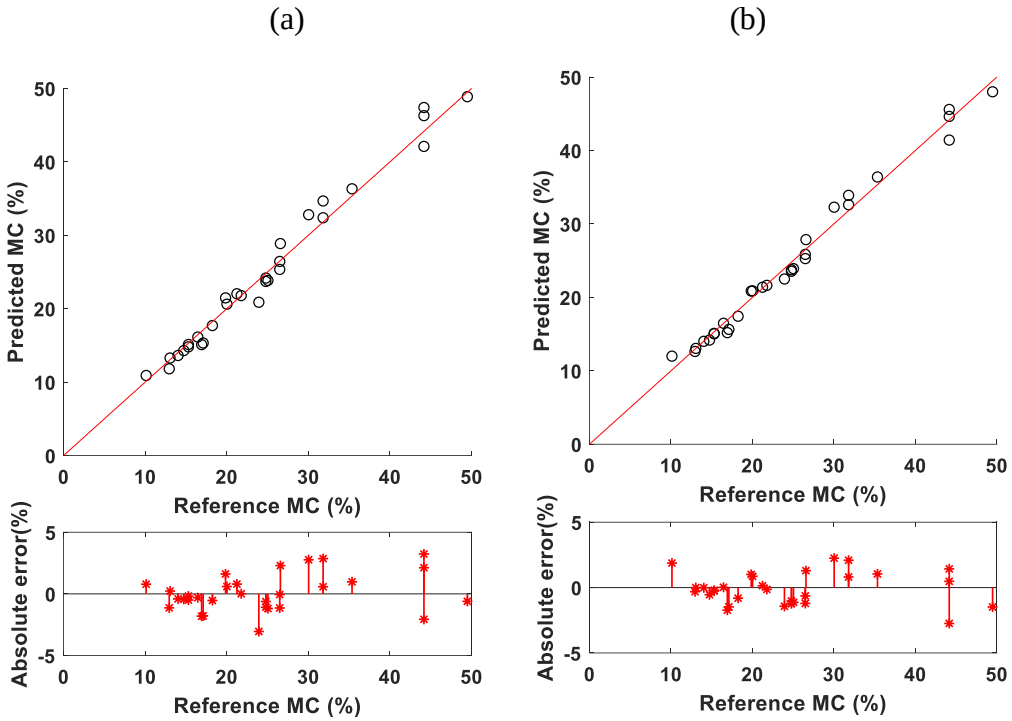

Fig. 12. Validation results of the data driven models. (a) DNN model. (b) RF model. (c) SVM model. (d) Proposed model.

Table 3. Performance of different data driven models

Model	R^2	RMSE(%)	MAE(%)	T(ms)
DNN	0.99	1.30	1.04	18.40
RF	0.96	2.23	1.64	13.51
SVM	0.98	1.51	1.19	1.83
Proposed model	0.99	1.21	0.99	21.43

Moreover, the prediction time of different models are compared. The SVM model has the fastest prediction time, which is less than 2 ms. Due to the complexity of RF and DNN models, the prediction time are nearly 14 ms and 19 ms, respectively. The proposed model with a prediction time less than 22 ms is sufficient for the real time prediction of the MC in woodchips. Based on the results from the above investigations on the prediction accuracy and prediction time, the proposed model is adopted in the capacitive MC measurement.

The type and random distribution of woodchips in the sensor influence the capacitive MC measurement. The data from cedarwood with different sizes are used to verify the prediction of the

proposed model. The prediction results are given in Fig. 13 and Table 4. It is found that the proposed model can predict the MC in cedarwood with absolute error within ±5% and that the prediction accuracy is different for different particle sizes. Since the large sized cedarwood is packed more randomly in the sensor, the error of the proposed model from large samples is higher than those from small and medium samples. Moreover, as shown in Fig. 13 (a) to (c), 89.7%, 86.2% and 72.4% of prediction results have the absolute error within ±2%, respectively.

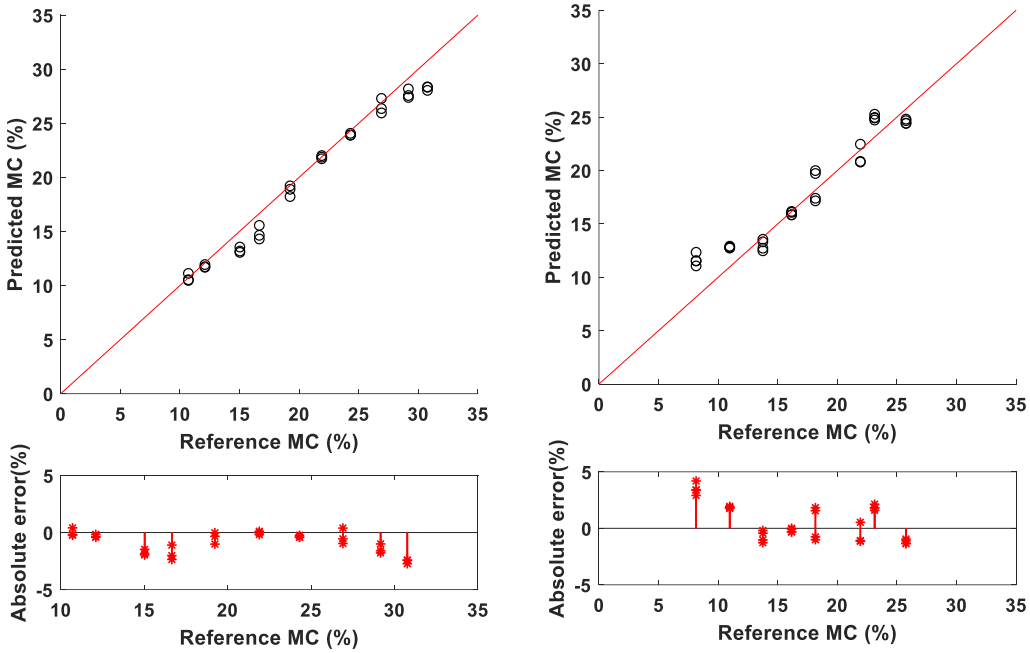

(a) (b)

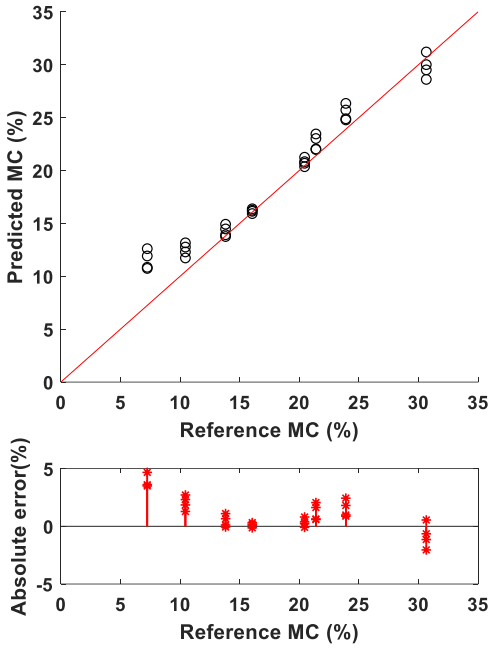

(c)

Fig. 13. Prediction results of cedarwood with different particle sizes. (a) Small samples. (b) Medium samples. (c) Large samples.

Table 4. Prediction results of cedarwood with different sizes

Particle size	R^2	RMSE(%)	MAE(%)
Small	0.98	1.30	0.97
Medium	0.96	1.75	1.40
Large	0.93	1.95	1.45

In addition, an empirical equation is also established. A second-order polynomial equation is selected due to the higher fitting accuracy. Based on the same training dataset with the proposed model, the coefficients of the equation are calculated using the least square method:

$$W_0 = 0.003m^2 - 0.023{C_1}^2 - 0.032{C_2}^2 + 0.865f^2 - 0.528m + 1.283C_1 + 0.535C_2 - 1.903f + 34.838 \quad (7)$$

where W_0 is the MC of the samples, m is the mass of the samples, C_1 and C_2 are the capacitance values at 300 kHz and 1 MHz, respectively, and f is the peak frequency of the capacitance spectrum. The prediction results of the empirical equation and the proposed model for the data from

cedarwood are plotted in Fig. 14. The generalization capability of two models is summarized in Table 5. Although the empirical equation has good accuracy on the training dataset, its generalization capability is not as good as the proposed model. In general, when the data from cedarwood are used as the validation dataset, the proposed model has good generalization capability with R^2, RMSE and MAE of 0.95, 1.69% and 1.28%, respectively. It is shown that the proposed system can be used to measure the MC in cedarwood with different particle sizes.

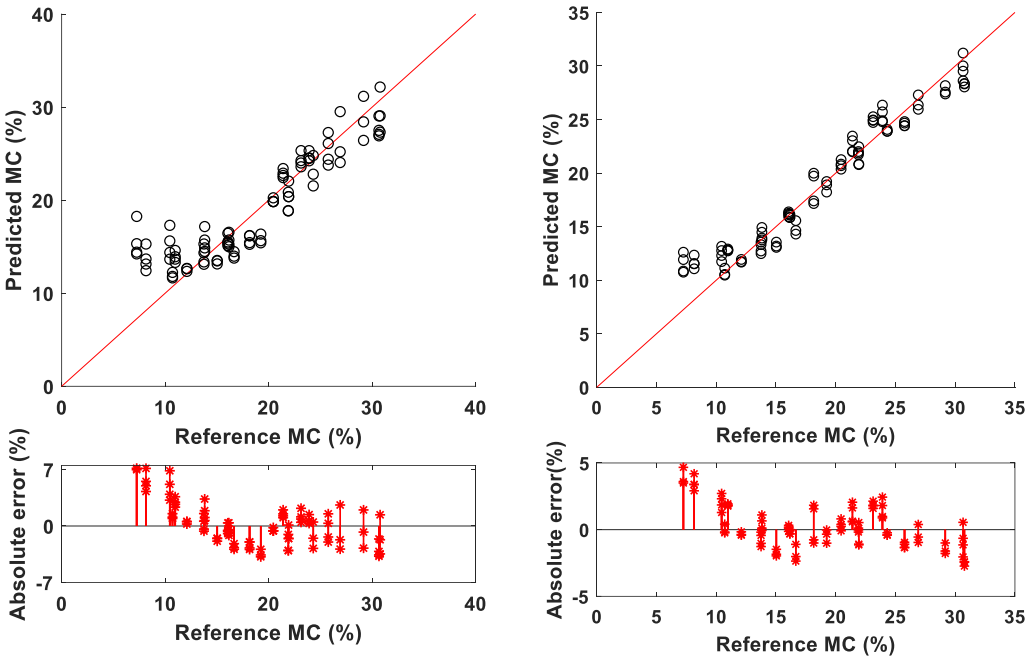

(a) (b)

Fig. 14. Prediction results for the data from cedarwood. (a) Empirical equation. (b) Proposed model.

Table 5. Generalization capability of empirical equation and proposed model

Models	R^2	RMSE(%)	MAE(%)
Empirical equation	0.82	2.95	2.21
Proposed model	0.95	1.69	1.28

Finally, two tests are conducted to investigate the uncertainty of the proposed system. Firstly, the predicted MC from the proposed model is calculated using the data from Fig. 6, which are measured under three repeated runs for the small sized cedarwood with the MC of 11.47%, 21.86% and

47.41%, respectively. Table 6 shows that the maximum discrepancy of the predicted MC from the three runs is less than 1.2%. Secondly, the other test is conducted with cedarwood for MC over the range 24.3% and 25.2%, as shown in Fig. 15. Although the packing density varies from 149.6 to 234.8 kg/m^3, the absolute error of the predicted MC is within ±2%. It is proved that the proposed measurement system can predict the MC in woodchips with remarkably different packing densities.

Table 6. MC measurement for three repeated runs

Data	First run	Second run	Third run
Fig. 6 (a)	12.62%	13.35%	13.11%
Fig. 6 (b)	21.84%	21.74%	21.65%
Fig. 6 (c)	46.87%	45.76%	45.70%

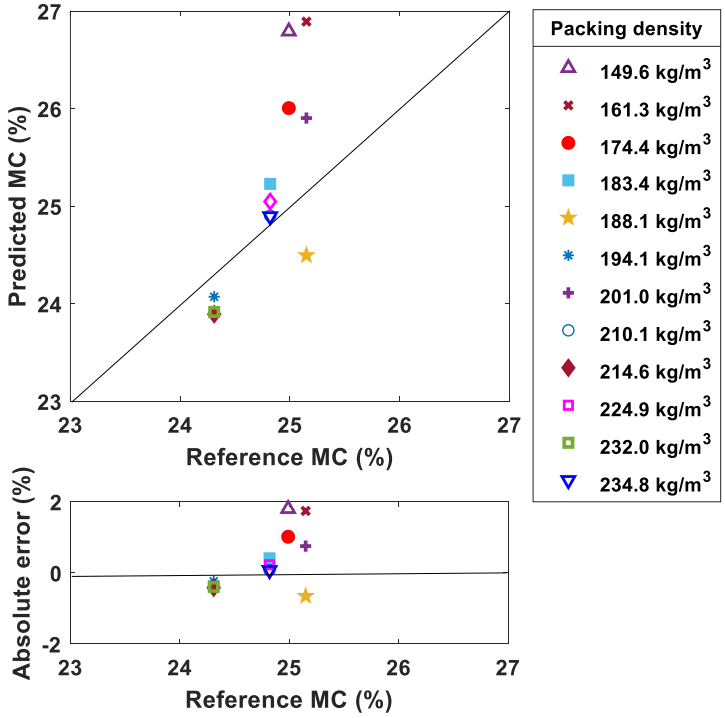

Fig. 15. Uncertainty of the measurement system for different packing densities of cedarwood.

5. Conclusions

A method for measuring the MC in woodchips using a helical capacitive sensor has been proposed. Through the investigations, the following conclusions are drawn:

1) By considering the non-uniformity of the sensitivity distribution and the practicality of the helical sensor, the optimal structural parameters of the electrodes are determined. In the optimal design of electrodes, the *L/D*, θ, *A/D* and *B/D* are set to 3, 110 °, 0.6 and 0.5, respectively, and these yield the sensing field non-uniformity (S_r) of 0.32.

2) By investigating the characteristics of the capacitance spectrum and the influence of the type and random distribution of woodchips in the sensor, the mass of the sample, the frequency at the peak of the capacitance spectrum and the capacitance values at 300 kHz and 1MHz are selected to be the input of data driven models.

3) Experimental results have proved that the proposed system can measure the MC in woodchips with absolute error within ±5% when the MC ranges from 7% to 49%. In addition, the proposed system has good generalization capability with R^2, RMSE and MAE of 0.95, 1.69% and 1.28%, respectively, in predicting the MC in cedarwood with different particle sizes. Moreover, the uncertainty of the proposed system with cedarwood over the range 24.3% and 25.2% has been quantified. Although the packing density varies from 149.6 to 234.8 kg/m^3, the absolute error of the predicted MC is within ±2%.

Woodchips may contain impurities such as clay, stone, etc. The quantitative evaluation of impurities on the proposed method will be investigated in the near future.

Acknowledgment

The authors would like to acknowledge the National Natural Science Foundation of China (62073135), Beijing Natural Science Foundation (3202028) and Fundamental Research Funds for the Central Universities (2020MS015) for providing financial support for this research.

References

[1] J. Nyström, E. Dahlquist, Methods for determination of moisture content in woodchips for power plants-a review, Fuel 83 (2004) 773-779.

[2] J. Posom, A. Shrestha, W. Saechua, P. Sirisomboon, Rapid non-destructive evaluation of moisture content and higher heating value of Leucaena leucocephala pellets using near infrared spectroscopy, Energy 107 (2016) 464-472.

[3] S. Julrat, S. Trabelsi, Portable six-port reflectometer for determining moisture content of biomass material, IEEE Sens. J. 17 (2017) 4814-4819.

[4] M. S. McKeown, S. Trabelsi, S. O. Nelson, E. W. Tollner, Microwave sensing of moisture in flowing biomass pellets, Biosyst. Eng. 155 (2017) 152-160.

[5] S. Julrat, S. Trabelsi, In-line microwave reflection measurement technique for determining moisture content of biomass material, Biosyst. Eng. 188 (2019) 24-30.

[6] S. Roels, J. Carmeliet, Analysis of moisture flow in porous materials using microfocus X-ray radiography, Int. J. Heat Mass Tran. 49 (2006) 4762-4772.

[7] Y. Q. Mao, W. C. Xia, G. Y. Xie, Y. L. Peng, Rapid detection of the total moisture content of coal fine by low-field nuclear magnetic resonance, Measurement 155 (2020) 107564.

[8] F. Rahimi-Ajdadi, Y. Abbaspour-Gilandeh, K. Mollazade, R.P.R. Hasanzadeh, Development of a novel machine vision procedure for rapid and non-contact measurement of soil moisture content, Measurement 121 (2018) 179-189.

[9] U. Kaatze, C. Hübner, Electromagnetic techniques for moisture content determination of materials, Meas. Sci. Technol. 21 (2010) 082001.

[10] J. Davis, D. Matovic, A. Pollard, The performance of resistance, inductance, and capacitance handheld meters for determining moisture content of low-carbon fuels, Fuel 188 (2017) 254-266.

[11] C. Kandala, J. Sundaram, Nondestructive measurement of moisture content using a parallel-plate capacitance sensor for grain and nuts, IEEE Sens. J. 10 (2010) 1282-1287.

[12] X. Deng, H.N. Gu, L. Yang, H.F. Lyu, Y.G. Cheng, L.P. Pan, Z.J. Fu, L.Q. Cui, L. Zhang, A method of electrical conductivity compensation in a low-cost soil moisture sensing measurement based on capacitance, Measurement 150 (2020) 107052.

[13] X. Deng, L. Yang, Z.J. Fu, C. Du, H.F. Lyu, L.Q. Cui, L. Zhang, J. Zhang, B. Jia, A calibration-free capacitive moisture detection method for multiple soil environments, Measurement 173 (2021) 108599.

[14] P. Chetpattananondh, K. Thongpull, K. Chetpattananondh, Interdigital capacitance sensing of moisture content in rubber wood, Comput. Electron. Agr. 142 (2017) 545-551.

[15] R. Dos Santos, J. Sallese, M. Mattavelli, A. Nunes, C. Dehollain, D. Barrettino, High precision capacitive moisture sensor for polymers: modeling and experiments, IEEE Sens. J. 20 (2020) 3032-3039.

[16] R. Dean, A. Rane, M. Baginski, J. Richard, Z. Hartzog, D. Elton, A capacitive fringing field sensor design for moisture measurement based on printed circuit board technology, IEEE Trans. Instrum. Meas. 61 (2012) 1105-1112.

[17] M. Goswami, B. Montazer, U. Sarma, Design and characterization of a fringing field capacitive soil moisture sensor, IEEE Trans. Instrum. Meas. 68 (2019) 913-922.

[18] P. Pan, T. McDonald, B. Via, J. Fulton, J. Hung, Predicting moisture content of chipped pine samples with a multi-electrode capacitance sensor, Biosyst. Eng. 145 (2016) 1-9.

[19] J. Ye, L. Peng, W. Wang, W. Zhou, Helical capacitance sensor based gas fraction measurement of gas-liquid two-phase flow in vertical tube with small diameter, IEEE Sens. J. 11 (2011) 1704-1710.

[20] J. Ye, L. Peng, W. Wang, W. Zhou, Optimization of helical capacitance sensor for void fraction measurement of gas-liquid two-phase flow in a small diameter tube, IEEE Sens. J. 11 (2011) 2189-2196.

[21] L. Lim, W. Pao, N. Hamid, T. Tang, Design of helical capacitance sensor for holdup measurement in two-phase stratified flow: a sinusoidal function approach, Sensors 16 (2016) 1032-1047.

[22] J. Li, D. Bi, Q. Jiang, H. Wang, C. Xu, Online monitoring and characterization of dense phase pneumatically conveyed coal particles on a pilot gasifier by electrostatic-capacitance-integrated instrumentation system, Measurement 125 (2018) 1-10.

[23] P. Kadlec, B. Gabrys, S. Strandt, Data-driven soft sensors in the process industry, Comput. Chem. Eng. 33 (2009) 795-814.

[24] J. Zhang, D. Du, Y. Bao, J. Wang, Z. Wei, Development of multifrequency-swept microwave sensing system for moisture measurement of sweet corn with deep neural network, IEEE Trans. Instrum. Meas. 69 (2020) 6446-6454.

[25] M. Malajner, D. Gleich, P. Planinsic, Soil type characterization for moisture estimation using machine learning and UWB-Time of Flight measurements, Measurement 146 (2019) 537-543.

[26] A. Ren, A. Zahid, A. Zoha, S. Shah, M. Imran, A. Alomainy, Q. Abbasi, Machine learning driven approach towards the quality assessment of fresh fruits using non-invasive sensing, IEEE Sens. J. 20 (2020) 2075-2083.

[27] L. Breiman, Random Forests, Mach. Learn. 45 (2001) 5–32.

[28] C. Shang, F. Yang, D. Huang, W. Lyu, Data-driven soft sensor development based on deep learning technique, J. Process. Contr. 24 (2014) 223-233.

[29] W. Yan, D. Tang, Y. Lin, A data-driven soft sensor modeling method based on deep learning and its application, IEEE T. Ind. Electron. 64 (2017) 4237-4245.

[30] X. Liu, Z. Zhang, Z. Song, A comparative study of the data-driven day-ahead hourly provincial load forecasting methods: From classical data mining to deep learning, Renew. Sust. Energ. Rev. 119 (2020) 109632.

[31] L. Rusiniak, Dielectric constant of water in a rock medium, Phys. Chem. Earth 23 (1998) 1133-1139.

[32] B. Shahriari, K. Swersky, Z. Wang, R. Adams, N. Freitas, Taking the human out of the loop: a review of bayesian optimization, P. IEEE 104 (2016) 148-175.